Effects of Separation Layer Thickness on Oxygen Permeation and Mechanical Strength of DL-HFMR-ScSZ

Zhentao Wu [1], Alan Thursfield [2], Ian Metcalfe [2] and K. Li [1,*]

1. Department of Chemical Engineering and Chemical Technology, Imperial College London, SW7 2AZ, U.K.
2. School of Chemical Engineering and Advanced Materials, Newcastle University, NE1 7RU, U.K.

Abstract

It has been demonstrated in our previous studies that in order for greater methane conversion and less coke-formation, a higher oxygen permeation rate through the outer oxygen separation layer of a functional dual-layer ceramic hollow fibre membrane is needed. Besides new membrane materials with higher oxygen permeability, another way of improving oxygen permeation is to reduce the separation layer thickness, although this strategy is limited by the characteristic thickness, L_c, where bulk diffusion and surface oxygen exchange are both important. As a result, a series of $La_{0.80}Sr_{0.20}MnO_{3-\delta}$ (LSM)-Scandia(10%)-Stabilized-Zirconia (ScSZ)/ScSZ-NiO functional dual-layer hollow fibres (DL-HF) with an outer oxygen separation layer thickness between approximately 8.0 and 72.4 μm were fabricated in this study, by using the single-step co-extrusion and co-sintering process. The effects of separation layer thickness on oxygen permeation and mechanical strength were investigated. The oxygen permeation of the LSM-ScSZ separation layer is more likely to be controlled by surface exchange at higher temperatures, and changes to mixed control by both bulk diffusion and surface exchange at lower temperatures. A thicker separation layer also results in a thinner catalytic substrate layer, and subsequently decreases the mechanical strength of the dual-layer hollow fibre membrane.

Key words: Oxygen permeation, co-extrusion and co-sintering, dual-layer ceramic hollow fibre, membrane reactor, methane conversion

*To whom correspondence should be addressed

Telephone: 44 (0) 207-5945676
Fax: 44 (0) 207-5945629
Email: Kang.Li@Imperial.ac.uk

1. Introduction

In our previous studies, a reliable membrane fabrication process, i.e. co-extrusion and co-sintering process, has been developed to fabricate dual-layer ceramic hollow fibre membranes with controlled structures. The membranes of this type have also been used as compact membrane reactors for methane conversion [1, 2] and micro-tubular solid oxide fuel cells (SOFC) [3-7]. With regard to the dual-layer hollow fibre membrane reactor (DL-HFMR), oxygen permeation through the outer oxygen separation layer is the key factor for better methane conversion and less coke-formation, determining the performance of such a membrane reactor design for methane conversion.

Use of dense ceramic membranes with unique mixed ionic-electronic conducting (MIEC) properties to separate highly pure oxygen from air has been widely studied for several decades [8-10]. The oxygen permeation through such membranes relies on two processes, i.e. surface exchange on the membrane surface (feed side and permeate side) and bulk diffusion of oxygen ions through the membrane. As the slowest step predominantly determines the overall rate of oxygen permeation, it is important to know what the rate-determining or controlling step for oxygen permeation is in order to further improve the oxygen permeation flux [11-13].

In principle, oxygen permeation flux changes with membrane thickness in the way shown in Figure 1. When the membrane is much thicker than the characteristic membrane thickness (L_C), bulk diffusion is the controlling step and the oxygen permeation flux increases linearly with the inverse of the membrane thickness (L). The increase of oxygen permeation flux deviates from the straight dashed line when the membrane thickness approaches L_C, indicating that oxygen permeation is co-governed by both bulk diffusion and surface exchange processes, which is quite usual for most of the reported ceramic membranes for oxygen separation. Further decrease of L to a level that is much lower than L_C would not increase the oxygen permeation, as surface exchange becomes the controlling step.

If the thickness of the oxygen separation layer of a DL-HFMR is higher than its characteristic thickness, a thinner separation layer allows a higher permeation of oxygen and subsequently improves the reactor performance. As a result, a series of $La_{0.80}Sr_{0.20}MnO_{3-\delta}$ (LSM)-Scandia(10%)-Stabilized-Zirconia (ScSZ)/ScSZ-NiO functional dual-layer hollow fibres (DL-HF) have been fabricated in this study, by using the co-extrusion and co-sintering process. The thickness of the outer oxygen separation layer (LSM-ScSZ) can be reduced from approximately 72.4 to 8.0 μm. The effect of outer separation layer thickness on the oxygen permeation of LSM-ScSZ/Ni-ScSZ dual-layer hollow fibre membranes has been investigated, in order to outline the controlling step for oxygen separation. The effect of outer layer thickness on the mechanical strength, another important property of ceramic hollow fibre membrane, has also been studied. It should be noted here that, although the current study aims to investigate the oxygen permeation of DL-HFMR-ScSZ, a similar membrane fabrication process and membrane structure can be used for other ceramic materials that have been shown to have excellent oxygen permeability, in an effort to further improve their performance for oxygen separation.

2. Experimental

2.1 Materials

$La_{0.80}Sr_{0.20}MnO_{3-\delta}$ (LSM, NexTech Materials Ltd, 5.8 m^2/g), NiO (NexTech Materials Ltd, 5.2 m^2/g) and scandia(10%)-stabilized-zirconia (ScSZ, NexTech Materials Ltd, 9.4 m^2/g) were used as supplied. Polyethersulfone, (PESf, Radel A-300, Ameco Performance, USA), Dimethyl Sulfoxide (DMSO, Sigma, >99.5%) and Arlacel P135 (Uniqema, UK) were used as polymer binder, solvent and additive functioning as dispersant respectively. DI water and tap water were used as the internal and the external coagulants, respectively, when fabricating the dual-layer hollow fibres.

2.2 Fabrication of LSM-ScSZ/NiO-ScSZ dual-layer hollow fibres

The preparation of spinning suspensions as well as the co-extrusion process has been described elsewhere [1, 2]. The outer oxygen permeation layer

consisted of 40 vol. % of LSM as an electronic conducting phase and 60 vol. % of ScSZ as an ionic conducting phase, while the inner catalytic substrate was made of a mixture of NiO and ScSZ. In contrast with the previous membrane fabrication process where the extrusion rates of both the inner and outer layers were fixed, the extrusion rate of the inner layer was maintained at a certain value for the work described in this study, while the extrusion rate of the outer layer was varied from 0.5 to 5 ml/min, resulting in a series of dual-layer hollow fibre membranes with gradually increased outer layer thicknesses. Table 1 lists the suspension compositions and co-extrusion parameters. The formed precursor fibres were then cut into the required length, dried and straightened, and finally co-sintered at 1400 °C for 5 h, with heating and cooling rates of 5-10 and 3 °C/min respectively.

2.3 Characterisation of dual-layer hollow fibres

The microstructure of the dual-layer hollow fibres was ascertained using a scanning electron microscope (SEM, JEOL JSM-5610LV, Tokyo, Japan). Mechanical strength was examined by three point bending tests (Tinius Olsen H25KS). Samples of around 5.0 cm in length were fixed on a sample holder with a 3.0 cm gap. The bending strength (σ_F, MPa) is calculated using the following equation:

$$\sigma_F = \frac{8 \cdot F \cdot L \cdot D}{\pi (D^4 - d_i^{\,4})} \tag{1}$$

where F is the measured loading at which fracture occurred (N); L, D, d_i are the length (m), the outer diameter and the inner diameter of the hollow fibres (m), respectively. In order to compare the mechanical strength of the co-sintered fibres and the one reduced in hydrogen for oxygen permeation and methane conversion measurements, some co-sintered fibres were cut into 5.0 cm in length, packed in a dense alumina tube and reduced separately in hydrogen (600 °C, 15 ml/min) for 30 min prior to mechanical strength tests.

2.4 Oxygen permeation and methane conversion of DL-HFMR-ScSZ

Measurements of oxygen permeation and methane conversion were carried out using the set-up shown in Figure 2. For oxygen permeation measurements, a dual-layer ceramic hollow fibre of approximately 11 cm in length was sealed between two dense alumina tubes (ID 2 mm, OD 4 mm) by high temperature ceramic sealant (RESBOND 940 LE, COTRONICS CORPORATION), and put in a CARBOLITE tubular furnace (15 cm in length, 5 cm of heating zone). Prior to the measurements, the inner layer was reduced in a hydrogen stream (15 ml/min) at 600 °C for 30 min and turned into a highly porous structure. A gas mixture of CO (10%)/Ar (20 ml/min) was used as the "sweep gas" for the oxygen permeation measurement, and the amount of oxygen permeated through the outer layer was monitored by the amount of CO_2 produced. N_2 of approximately 1×10^{-3} ml/s was detected by GC before the measurement, which is very similar to our previous studies [1, 2]. Such a low level of leakage did not change during the whole measuring processes, indicating good gas tightness of the separation layer.

Measurements of methane conversion were performed as in previous studies [1, 2]. After reduction of the inner layer, 20 ml/min of CH_4(10%)/Ar was fed into the lumen of the fibre, while the outer surface was exposed to ambient air inside the furnace. Methane conversion (X_{CH4}, %) and S_C (%) indicating the methane converted into coke and possibly tiny amounts of C2 products were calculated using the following equations, while oxygen permeation rate (F_{O2}, ml/min) was calculated based on the mass balances of oxygen.

$$X_{CH_4} = \frac{F_{CH_4 inlet} - F_{CH_4 outlet}}{F_{CH_4 inlet}} \times 100\% \quad (1)$$

$$S_c = (1 - \frac{F_{CO} + F_{CO_2}}{F_{CH_4 inlet} - F_{CH_4 outlet}}) \times 100\% \quad (2)$$

3. Results and discussion

3.1 Morphology of the precursor dual-layer hollow fibres

Figure 3 shows photographic images of the precursor dual-layer fibres, with the outer layer extrusion rate varied from 0.5 to 5.0 ml/min. As can be seen, the inner catalytic substrate layer is of a typical asymmetric structure, i.e. a sponge-like layer supported on another finger-like layer, while the outer oxygen separation layer is of sponge-like structure. Furthermore, there is a clear interface between the two layers, with the outer layer tightly bonded to the inner layer with no gaps between them, indicating good uniformity of the prepared fibres and great adhesion between the two layers.

It can also be seen in Figure 3 that the thickness of the outer oxygen separation layer increases with increasing extrusion rate, while the asymmetric structure of the inner catalytic substrate layer is only weakly affected. This also demonstrates that the co-extrusion process provides a controlled way of fabricating dual-layer ceramic hollow fibres, especially with respect to reducing the thickness of the separation layer (the top-layer) while maintaining sufficient membrane uniformity. Currently this is not guaranteed using most other multi-step membrane fabrication processes, especially for membranes in the form of hollow fibre or micro-tubes.

3.2 Microstructure of the co-sintered dual-layer hollow fibres

Figures 4-9 show the microstructures of the co-sintered hollow fibres with different outer layer thicknesses. As can be seen in Figure 4, all the co-sintered samples are of uniform hollow fibre configuration and consist of a symmetric outer layer supported on an asymmetric inner layer. The morphology is very similar to the precursor fibres, except for the smaller inner and outer diameters due to shrinkage at high sintering temperatures (1400 °C). The change in the outer layer thickness with the different extrusion rates is shown in Figure 5, in which a clear interface between the two layers can be seen due to the different textures of each individual layer. Although the thickness of the outer layer keeps increasing with its extrusion rate, the two layers are always closely bound together, indicating great adhesion between the two layers at high temperatures. Both the inner and outer layers are densified after co-sintering (Figures 6 and 7) and there is little change in the microstructure of the two layers except for the variation of the outer layer

thickness. Similarly, the microstructures of both the inner surface and the outer surface change little with the different outer layer thickness, as shown in Figures 8 and 9. The presence of surface pores in Figure 9 agrees with the previous study [1] and has been proved that it would not affect the gas-tightness of the separation layer.

As a result, it can be concluded that the variation of the extrusion rate of the outer layer during the co-extrusion process would not change the microstructure of the resultant dual-layer hollow fibres, except for the thickness of the two layers. The inner diameter (ID) and outer diameter (OD) of the co-sintered dual-layer hollow fibres with different outer layer thicknesses are very similar, and are approximately 750 and 1300 μm, respectively, observed by SEM. The thickness of the inner layer decreases with increasing outer layer extrusion rate (from 0.5 to 5.0 ml/min), while the thickness of the outer layer increases (Figure 10). This results in a significant drop in the ratio between the thickness of the inner and the outer layers, especially when the outer layer is very thin (from 0.5 to 2.0 ml/min). When the extrusion rate is increased from 2.0 to 5.0 ml/min, the drop in the thickness ratio is less pronounced. Such a change in the thicknesses of the two layers with the varied extrusion rate of the outer layer is due to the co-extrusion process. The current co-extrusion process is based on the conventional dry-wet spinning method that has been widely used to fabricate polymer and ceramic hollow fibre membranes. In this process, there is an air gap between the spinneret and the external coagulation bath (it is called wet spinning when the air gap is zero, or the spinneret is immersed in the external coagulation bath). In order to obtain a fully symmetric structure of the outer layer, a large air gap of 26 cm must be used. Otherwise, finger-like voids will also develop from the outer surface and will sometimes penetrate through the boundary between the two layers. Such finger-like voids can be considered as defects in the outer oxygen separation layer and consequently can adversely affect the gas-tightness and mechanical properties of this layer, although the resistance of bulk diffusion may be reduced as well.

The use of a large air gap means that the spinning suspension extruded through the spinneret has to pass a vertical distance of 26 cm, prior to making contact with the external coagulation bath where the phase inversion is completed. With this air gap length, the phase inversion process is incomplete in the region between the spinneret and the coagulation bath and as a result the precursor fibre is soft. When the extrusion rate of the outer layer is increased (the rate of the inner layer is maintained stable by the syringe pump), the precursor fibre in the air gap becomes heavier, which causes plastic deformation of the fibre and subsequently reduces the thickness of the inner layer. As the increased extrusion rate of the outer layer is able to compensate for this phenomenon of deformation, the thickness of the outer layer still increases with increasing extrusion rate.

Due to the change in the thicknesses of the two layers as the outer layer extrusion rate is varied, the mechanical strength of the resultant membranes is affected and is investigated in the following section.

3.3 Mechanical strength of the dual-layer hollow fibres

Figure 11 shows how the mechanical strength of the developed dual-layer hollow fibres as a function of thickness of the two layers. As can be seen, the mechanical strength of the co-sintered fibres (before reduction in hydrogen) is reduced with decreasing thickness of the inner layer (or increasing thickness of the outer layer), which indicates that the major contribution to the mechanical strength of the dual-layer hollow fibre is from the inner layer, in agreement with previous studies [2]. After reduction, the NiO in the inner layer is converted into Ni and the dense inner layer turns into a highly porous structure. This reduces the mechanical strength of the dual-layer hollow fibre by around 25%. Meanwhile, the major contribution to the mechanical strength of the reduced dual-layer hollow fibres should also be from the inner layer, as strength decreases with decreasing thickness of the inner layer (or increasing thickness of the outer layer). Furthermore, the drop in the mechanical strength of both the co-sintered and the reduced samples decreases in a more moderate way when the extrusion rate of the outer layer is increased from 2.0

to 5.0 ml/min, in agreement with the change of the thickness ratio between the two layers.

3.4 Oxygen permeation of the dual-layer hollow fibre membranes

Oxygen permeation of the LSM-ScSZ/Ni-ScSZ dual-layer hollow fibre membranes was investigated using the set-up shown in Figure 2. Direct measurement of oxygen permeation using inert sweep gas would result in the re-oxidation of Ni into NiO by the permeated oxygen. This would result in significant changes in mass transfer resistance of the inner layer during the measurement. As a result, a gas mixture of CO (10%)/Ar (20 ml/min) was used to maintain the porous structure of the inner layer, by efficiently consuming the permeated oxygen. At each temperature point, the measurement was continued for at least 30 min when there were no changes in CO or CO_2 concentrations. No additional O_2 was detected by GC during the whole measurement, indicating that all the permeated O_2 was consumed by CO. The oxygen permeation rate can be calculated from the amount of CO_2 formed. Three membranes with outer layer extrusion rates of 0.5, 2.0 and 5.0 ml/min were tested, thicknesses of the outer oxygen separation layer being 8.0, 34.5 and 72.4 μm, respectively.

As can be seen in Figure 12, for all the membranes tested, the oxygen permeation increases with elevated operating temperatures. When the operating temperature is below 920 °C, the oxygen permeation rate increases with decreasing thickness of the outer separation layer, which indicates that bulk diffusion determines or co-determines the oxygen permeation. While at 970 °C, oxygen permeation rates of all the three membranes were almost identical, indicating that at or above this temperature surface exchange is the controlling step for oxygen permeation. Further reduction in the thickness of the separation layer would not increase the oxygen permeation rate in this case. As the inner layer is highly porous after reduction, its mass transfer resistance can be neglected when compared with the resistance from the separation layer. Although the inner layer thicknesses of the three tested membranes are slightly different, it is reasonable to assume that such a change in oxygen permeation rate (Figure 12) is predominantly due to the

varying thicknesses of the outer oxygen separation layer. As a result, bulk diffusion is more likely to be the controlling step for oxygen permeation at lower operating temperatures, while surface exchange is the controlling step at higher temperatures.

The effects of separation layer thickness on oxygen permeation at different temperatures can also be presented in the way shown in Figure 1. As can be seen in Figure 13, at 970 °C, surface exchange is always the controlling step for oxygen permeation because the oxygen permeation rate does not change with the separation layer thickness (between 8.0 and 72.4 μm). This indicates that the value of L_c at this temperature is significantly higher than 72.4 μm. While at 920 °C, oxygen permeation of the membrane with a separation layer thickness of 72.4 μm should be co-determined by bulk diffusion and surface exchange, i.e. the mixed control range in Figure 1. Pure surface exchange control only occurs when the separation layer is less than 34.5 μm. At lower operating temperatures (870 and 820 °C), oxygen permeation of the membrane with a separation layer thickness of 34.5 μm shifts into the co-determining range, while the sample with a 72.4 μm separation layer moves further towards bulk diffusion control although it may still be within the mixed control region. This indicates that, for the LSM-ScSZ/Ni-ScSZ dual-layer hollow fibre membranes, the value of L_c increases with temperature, and as a result, oxygen permeation of the 72.4 μm separation layer is controlled by surface exchange processes at 970 °C. As the value of L_c decreases at lower temperatures, oxygen permeation for the same separation layer thickness shifts towards the bulk diffusion control when the temperature is reduced to 820 °C. Such oxygen permeation behaviour is in agreement with a number of previous studies. Bouwmeester et. al. [14, 15] collected and compared the values of D_a (ambi-polar diffusion coefficient) and K_s (surface exchange coefficient) of a series of perovskite-type oxides obtained by O^{18}-O^{16} isotope exchange techniques and concluded that L_c changes with different dopant concentrations with a slight tendency for L_c to increase at elevated temperatures. Also, there is a wide range of the values for L_c from 20 to 3000

μm at 900 °C for different perovskite-type oxides, indicating the importance of surface exchange for oxygen permeation through MIEC membranes. Hong et. al. [16] investigated the oxygen permeation of $Ba_{0.5}Sr_{0.5}Co_{0.8}Fe_{0.2}O_{3-\delta}$ (BSCF) between 750 and 900 °C, with and without a $La_{0.7}Sr_{0.3}CoO_{3-\delta}$ (LSC) coating layer for different surface exchange processes. Besides higher oxygen permeation, L_c of the LSC-coated BSCF membrane was about half that of the uncoated counterparts. Furthermore, L_c of both LSC-coated and uncoated BSCF membranes increase with increasing temperatures from 800 to 900 °C. This indicates that with decreasing membrane thickness or increasing temperature, oxygen permeation of BSCF is more likely to be controlled by surface exchange processes. Chen et. al. [17] investigated the oxygen permeation of $La_{0.7}Sr_{0.3}CoO_{3-\delta}$ (LSC) membranes and the value of L_c increased from 68±20 to 87±21 μm when the temperature was elevated from 1000 to 1100 °C. However, there are other studies showing different conclusions. Tan et. al. [18-20] investigated the oxygen permeation of an $La_{0.6}Sr_{0.4}Co_{0.2}Fe_{0.8}O_{3-\delta}$ (LSCF) hollow fibre membrane and concluded that the controlling step changes from surface exchange processes at lower operating temperatures to bulk diffusion at higher temperatures. Furthermore, other studies have proved that the value of L_c changes with the composition of the membrane material [21, 22].

In terms of dense ceramic membranes made of dual-phase materials for oxygen separation, its mechanism of oxygen permeation is less well studied and described when compared with the one made of single phase materials with the perovskite structure. Oxygen transport in a dense membrane made of LSM-yttria-stabilised zirconia (YSZ) was studied by the group of Kilner [23, 24]. Both oxygen diffusion and surface exchange increase with elevating temperatures, which is same as the single-phase materials. Interestingly, surface exchanges of such dual-phase materials were higher than LSM and YSZ, while a higher content of LSM resulted in lower oxygen diffusion. For a disk-type sample (LSM-YSZ, 35-65 wt.%), surface exchange coefficient increased with elevated temperatures (from 803 to 995 °C) in a much faster

way than oxygen diffusion, which may indicate that bulk diffusion is more likely to be the controlling step at higher operating temperatures.

The oxygen permeation of the LSM-ScSZ separation layer may not be directly compared with the single phase MIEC membranes and the disk-type LSM-YSZ dual-phase membrane (due to different surface exchange processes). However, by using the principles of oxygen permeation through the dense ceramic membranes, the controlling step of oxygen permeation through LSM-ScSZ should be more likely to be surface exchange controlled at higher operating temperatures or for thinner LSM-ScSZ separation layers. Also, by using the co-extrusion and co-sintering process for membrane fabrication, the thickness of the oxygen separation layer can be reduced to several microns, and surface exchange can easily be the controlling step for oxygen permeation. If the same knowledge and techniques can be transferred to the fabrication of other oxygen permeation membranes, significantly higher oxygen permeation can be expected.

Since surface exchange of LSM-ScSZ is the controlling step for oxygen permeation at high operating temperatures, and high temperatures have to be used in order to increase oxygen permeation and subsequently improve the performance of the DL-HFMR [1, 2], it is reasonable to predict that the maximum achievable methane conversion of all DL-HFMR-ScSZ with different thicknesses of the outer oxygen separation layer will be the same. However, for completeness, two DL-HFMR-ScSZ with outer oxygen separation layers of 8.0 and 63.8 μm were tested for methane conversion at 820 °C. The purpose of this test is to confirm that thinner separation layers still contribute to improving reactor performance at lower operating temperatures where bulk diffusion co-determines the oxygen permeation.

Two dual-layer hollow fibres (14 cm in length) of the same outer layer thickness were bundled together and used as a DL-HFMR-ScSZ for methane conversion This was done with the aim of achieving sufficient membrane surface area, and as a result, a higher oxygen permeation rate. As can be seen in Figure 14, under the same operating conditions, the trends in the

changes in methane conversion, coke formation and oxygen permeation rate with reaction time are in agreement with previous studies [1, 2]. The DL-HFMR-ScSZ with a thinner oxygen separation layer (8.0 μm) shows higher methane conversion and oxygen permeation rate, together with less coke formation, when compared to the one with a thicker oxygen separation layer (63.8 μm). This also agrees with the oxygen permeation measurement shown in Figures 12 and 13, in which bulk diffusion co-determines oxygen permeation at lower operating temperatures.

4. Conclusions

In this study, a series of LSM-ScSZ/NiO-ScSZ dual-layer hollow fibres with outer oxygen separation layers of approximately 8.0 to 72.4 μm have been fabricated using the single-step co-extrusion and co-sintering process. The change in the outer layer thickness can be achieved by varying the extrusion rate of the outer layer while maintaining the rate of the inner layer. This results in thicker outer layers and thinner inner layers as the extrusion rate of the outer layer is increased. As the major contribution to the mechanical strength of such dual-layer hollow fibres is from the inner substrate layer, the fibre with a thicker outer layer is weaker as a result of an increase in the extrusion rate of the outer layer leading to a reduction in the thickness of the inner layer. The oxygen permeation of such fibres is co-determined by both bulk diffusion and surface exchange at lower operating temperatures, while surface exchange becomes the controlling step at higher temperatures. Based on the previous studies, developing new dual-phase membrane materials with higher oxygen permeability is the key step in further improving the performance of DL-HFMR design for methane conversion. In addition, as a new membrane fabrication process, the advantages of the single-step co-extrusion and co-sintering process have been demonstrated. Its potential in developing more advanced ceramic membranes with specific functions has also been demonstrated.

Acknowledgement

The authors would like to acknowledge financial support by the EPSRC (grant No: EP/G012679/1) for financial support.

References

1. Wu ZT, Wang B, Li K. Functional LSM-ScSZ/NiO-ScSZ dual-layer hollow fibres for partial oxidation of methane. International Journal of Hydrogen Energy 2011; 36 (9): 5334-5341.

2. Wu ZT, Wang B, Li K. A novel dual-layer ceramic hollow fibre membrane reactor for methane conversion. Journal of Membrane Science 2010; 352 (1-2): 63-70.

3. Othman MHD, Wu ZT, Droushiotis N, Doraswami U, Kelsall G, Li K. Single-step fabrication and characterisations of electrolyte/anode dual-layer hollow fibres for micro-tubular solid oxide fuel cells. Journal of Membrane Science 2010; 351 (1-2): 196-204.

4. Othman MHD, Droushiotis N, Wu ZT, Kelsall G, Li K. High-Performance, Anode-Supported, Microtubular SOFC Prepared from Single-Step-Fabricated, Dual-Layer Hollow Fibers. Advanced Materials 2011; 23 (21): 2480-+.

5. Othman MHD, Droushiotis N, Wu ZT, Kanawka K, Kelsall G, Li K. Electrolyte thickness control and its effect on electrolyte/anode dual-layer hollow fibres for micro-tubular solid oxide fuel cells. Journal of Membrane Science 2010; 365 (1-2): 382-388.

6. Kanawka K, Othman MHD, Wu ZT, Droushiotis N, Kelsall G, Li K. A dual layer Ni/Ni-YSZ hollow fibre for micro-tubular SOFC anode support with a current collector. Electrochemistry Communications 2011; 13 (1): 93-95.

7. Droushiotis N, Othman MHD, Doraswami U, Wu ZT, Kelsall G, Li K. Novel co-extruded electrolyte-anode hollow fibres for solid oxide fuel cells. Electrochemistry Communications 2009; 11 (9): 1799-1802.

8. Sunarso J, Baumann S, Serra JM, Meulenberg WA, Liu S, Lin YS, da Costa JCD. Mixed ionic-electronic conducting (MIEC) ceramic-based membranes for oxygen separation. Journal of Membrane Science 2008; 320 (1-2): 13-41.

9. Thursfield A, Metcalfe IS. The use of dense mixed ionic and electronic conducting membranes for chemical production. Journal of Materials Chemistry 2004; 14 (16): 2475-2485.

10. Liu YY, Tan XY, Li K. Mixed conducting ceramics for catalytic membrane processing. Catalysis Reviews-Science and Engineering 2006; 48 (2): 145-198.

11. Kim S, Yang YL, Jacobson AJ, Abeles B. Diffusion and surface exchange coefficients in mixed ionic electronic conducting oxides from the pressure

dependence of oxygen permeation. Solid State Ionics 1998; 106 (3-4): 189-195.

12. Virkar AV. Theoretical analysis of the role of interfaces in transport through oxygen ion and electron conducting membranes. Journal of Power Sources 2005; 147 (1-2): 8-31.

13. Kim S, Yang YL, Jacobson AJ, Abeles B. Oxygen surface exchange in mixed ionic electronic conductor membranes. Solid State Ionics 1999; 121 (1-4): 31-36.

14. Bouwmeester HJM, Kruidhof H, Burggraaf AJ. Importance of the Surface Exchange Kinetics as Rate-Limiting Step in Oxygen Permeation through Mixed-Conducting Oxides. Solid State Ionics 1994; 72 185-194.

15. Bouwmeester HJM, Burggraaf AJ, Cot AJBaL, *Chapter 10 Dense ceramic membranes for oxygen separation*, in *Membrane Science and Technology*. 1996, Elsevier. p. 435-528.

16. Hong WK, Choi GM. Oxygen permeation of BSCF membrane with varying thickness and surface coating. Journal of Membrane Science 2010; 346 (2): 353-360.

17. Chen CH, Bouwmeester HJM, vanDoorn RHE, Kruidhof H, Burggraaf AJ. Oxygen permeation of La0.3Sr0.7CoO3-delta. Solid State Ionics 1997; 98 (1-2): 7-13.

18. Tan XY, Liu YT, Li K. Mixed conducting ceramic hollow-fiber membranes for air separation. Aiche Journal 2005; 51 (7): 1991-2000.

19. Tan XY, Li K. Oxygen production using dense ceramic hollow fiber membrane modules with different operating modes. Aiche Journal 2007; 53 (4): 838-845.

20. Tan XY, Li K. Modeling of air separation in a LSCF hollow-fiber membrane module. Aiche Journal 2002; 48 (7): 1469-1477.

21. Geffroy PM, Bassat JM, Vivet A, Fourcade S, Chartier T, Del Gallo P, Richet N. Oxygen semi-permeation, oxygen diffusion and surface exchange coefficient of La((1-x))Sr(x)Fe((1-y))Ga(y)O(3-delta) perovskite membranes. Journal of Membrane Science 2010; 354 (1-2): 6-13.

22. Tenelshof JE, Bouwmeester HJM, Verweij H. Oxygen-Transport through La1-Xsrxfeo3-Delta Membranes .1. Permeation in Air/He Gradients. Solid State Ionics 1995; 81 (1-2): 97-109.

23. Dhallu M, Kilner JA. Oxygen transport in YSZ/LSM composite materials. Journal of Fuel Cell Science and Technology 2005; 2 (1): 29-33.

24. Ji Y, Kilner JA, Carolan MF. Electrical properties and oxygen diffusion in yttria-stabilised zirconia (YSZ)-La0.8Sr0.2MnO3 +/-delta (LSM) composites. Solid State Ionics 2005; 176 (9-10): 937-943.

Table 1. Compositions of spinning suspensions and co-extrusion parameters

	Suspension composition	
	Outer oxygen separation layer (wt.%)	Inner catalytic substrate layer (wt.%)
Ceramics	65.0	68.0
DMSO	28.0	24.7
PESf	6.5	6.8
Additive	0.5	0.5
	Co-extrusion parameters	
	Outer layer suspension	Inner layer suspension
Extrusion rate (ml/min)	0.5 – 5.0	8.0
Temperature (°C)	20	
Air gap (cm)	26	
Internal coagulant (ml/min)	10	

List of figures

8.0 μm (blank symbols) and 63.8 μm (solid symbols) at 820 °C

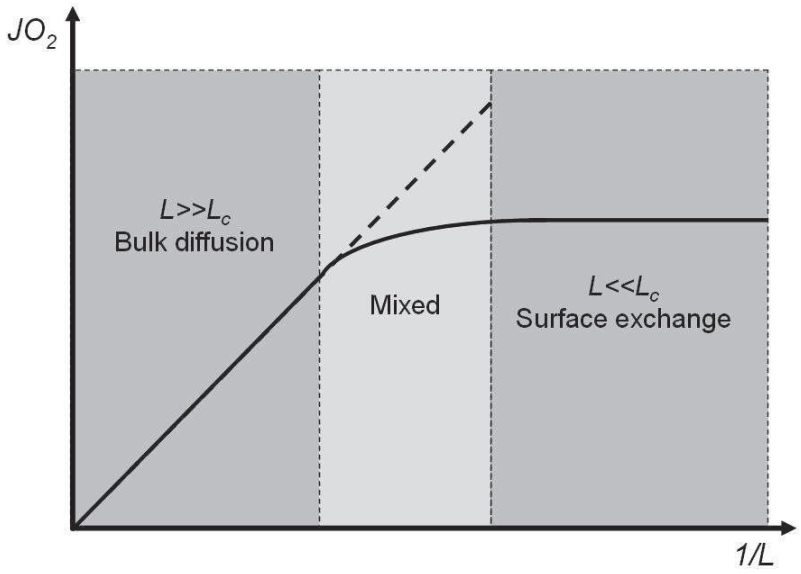

Figure 1

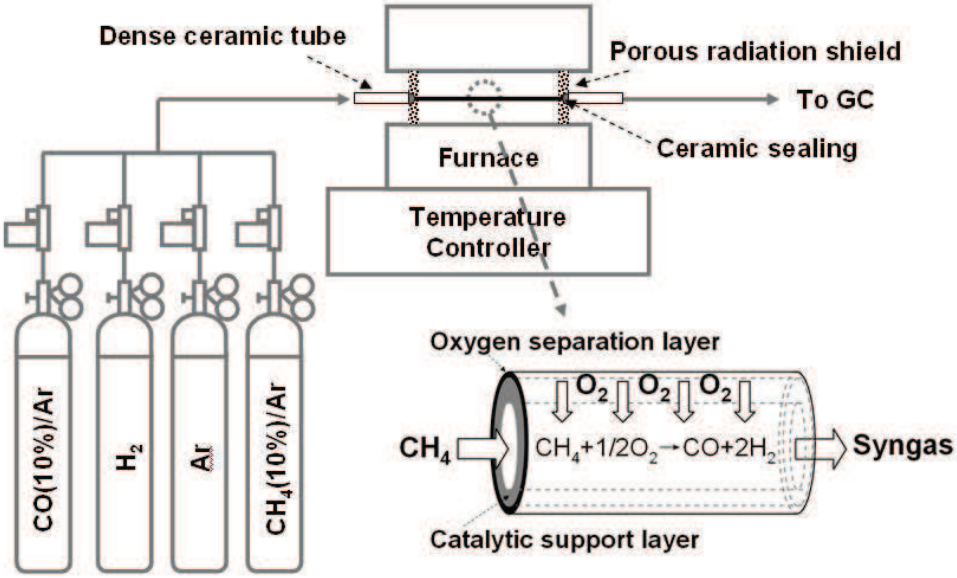
Dense ceramic tube
Porous radiation shield
To GC
Ceramic sealing
Furnace
Temperature Controller
CO(10%)/Ar
H2
Ar
CH4(10%)/Ar
Oxygen separation layer
O2 O2 O2
CH4
CH4+1/2O2→CO+2H2
Syngas
Catalytic support layer

Figure 2

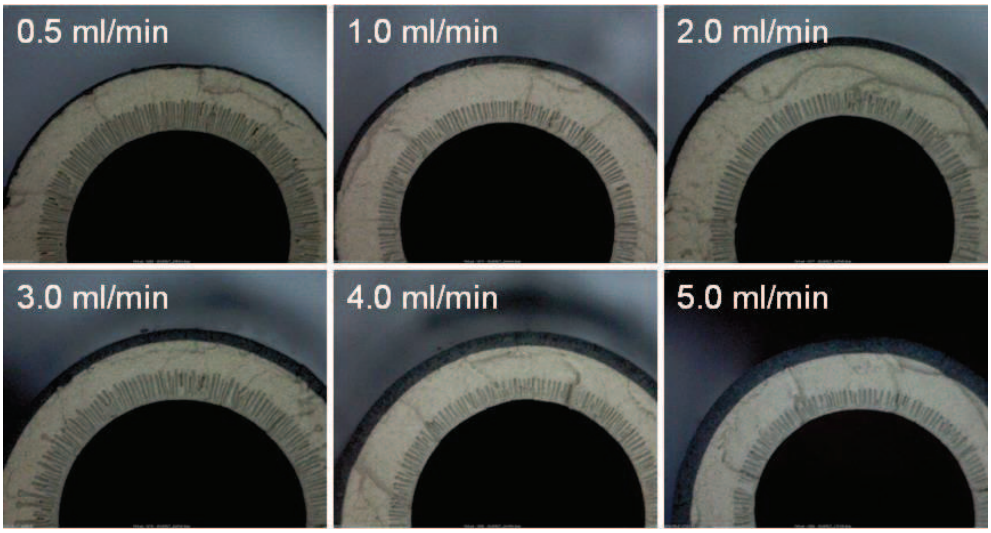

Figure 3

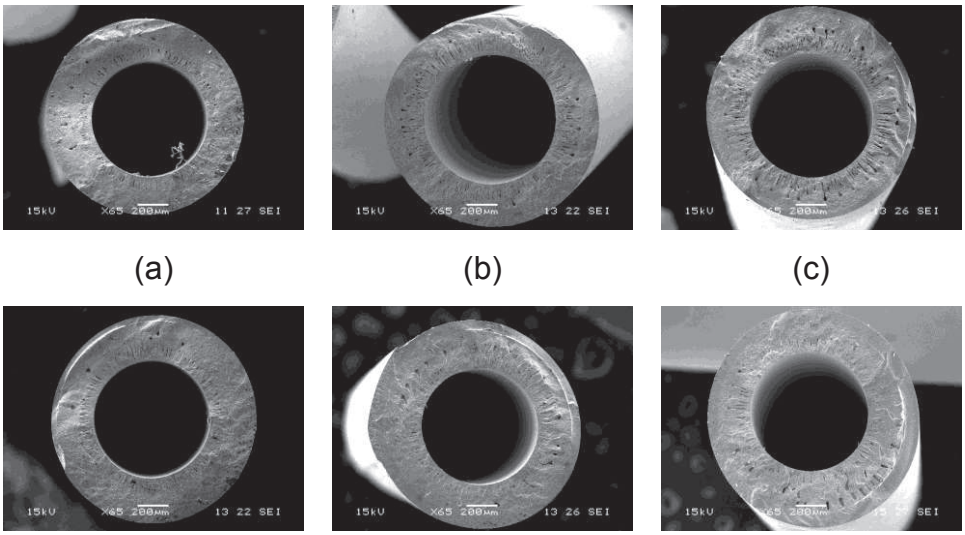

(a) (b) (c)

(d) (e) (f)

Figure 4

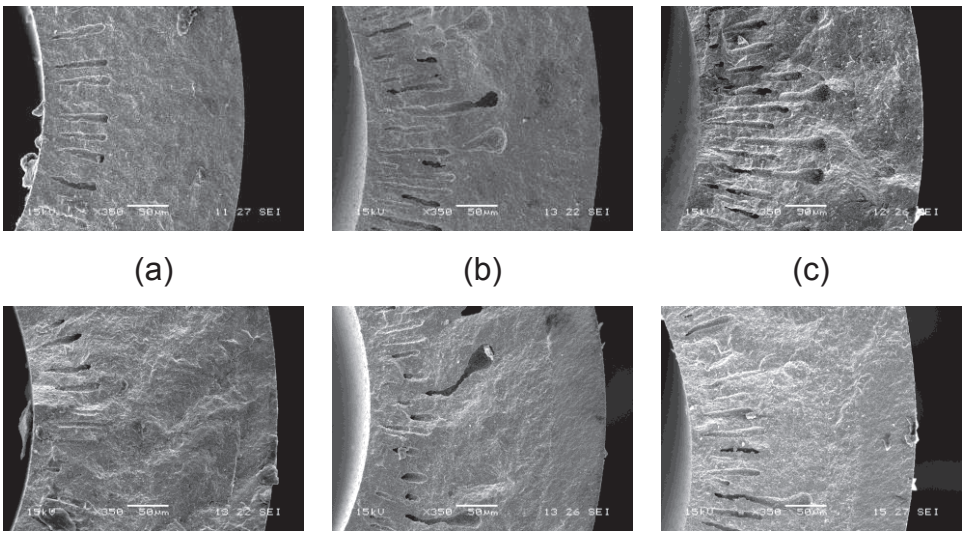

(a) (b) (c)

(d) (e) (f)

Figure 5

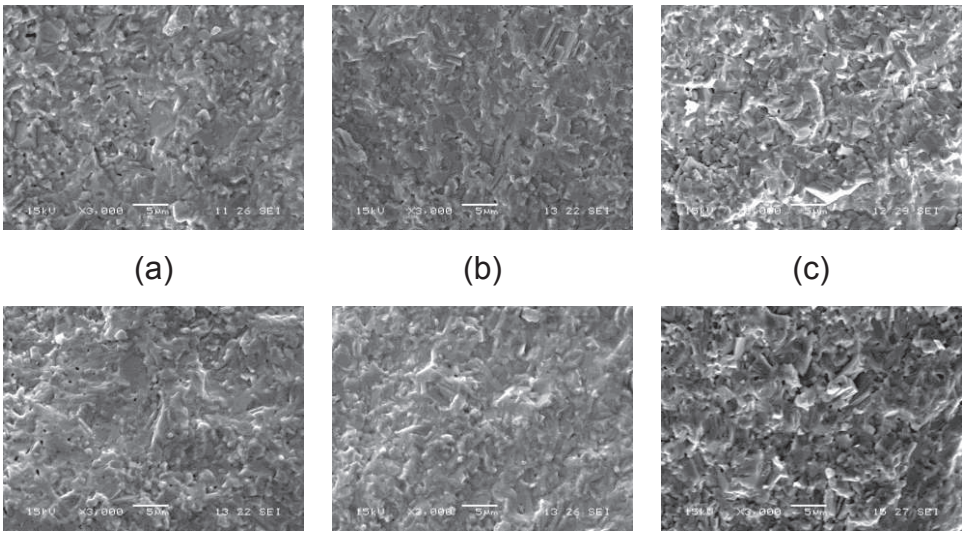

(a) (b) (c)

(d) (e) (f)

Figure 6

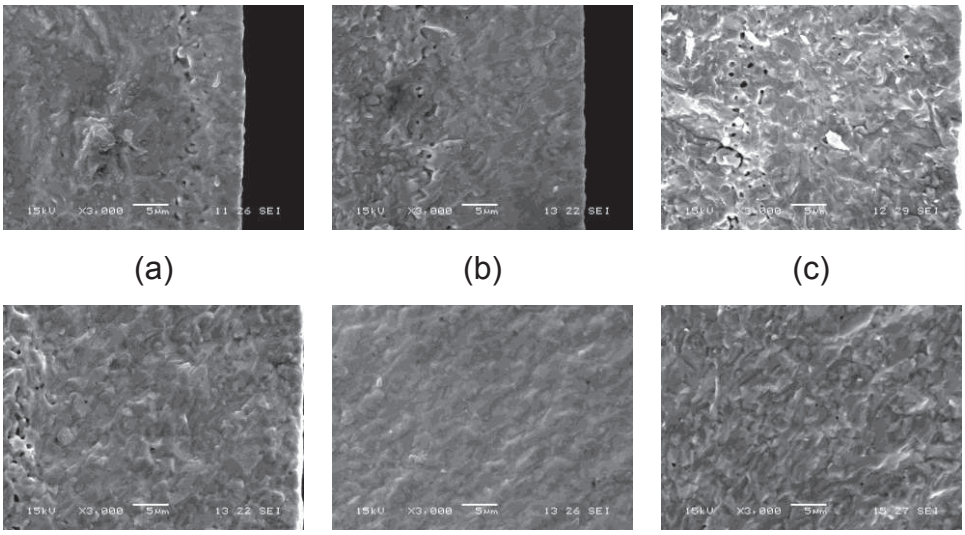

(a) (b) (c)

(d) (e) (f)

Figure 7

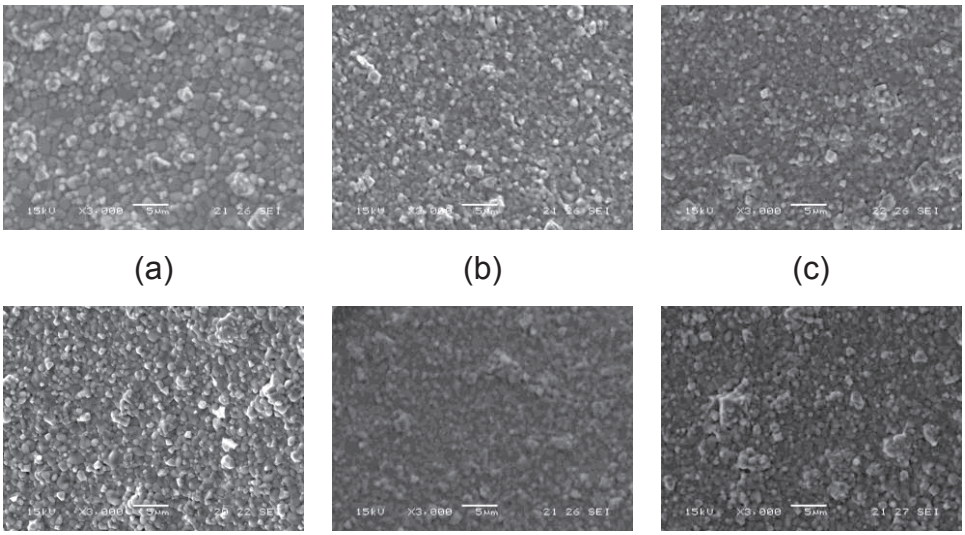

(a) (b) (c)

(d) (e) (f)

Figure 8

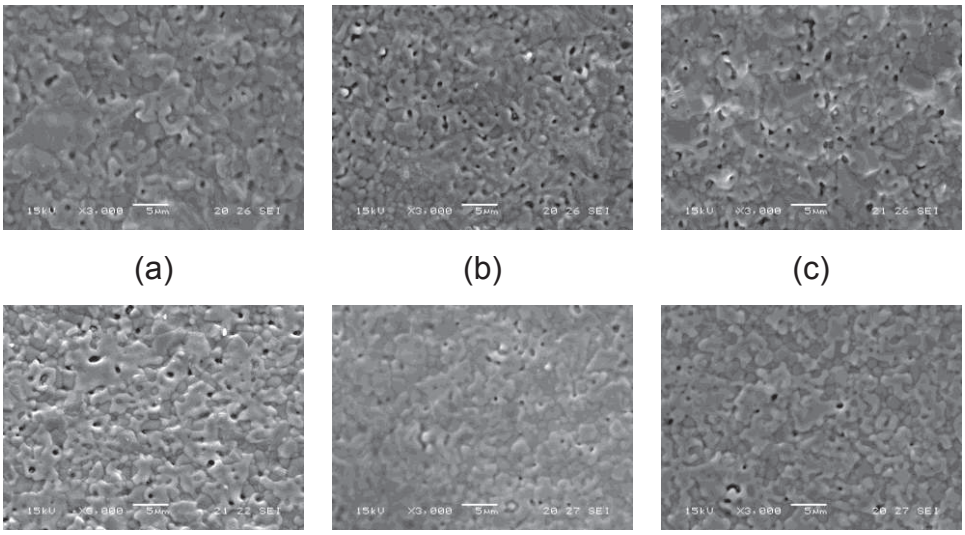

(a) (b) (c)

(d) (e) (f)

Figure 9

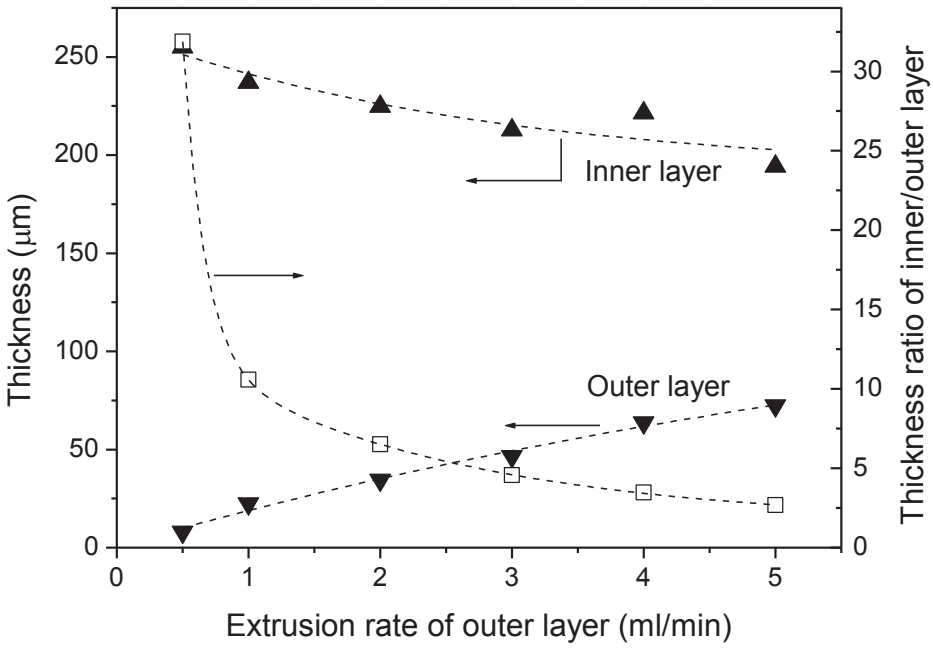
Thickness (μm)
Thickness ratio of inner/outer layer
Extrusion rate of outer layer (ml/min)
Inner layer
Outer layer
0
50
100
150
200
250
0
5
10
15
20
25
30
0
1
2
3
4
5

Figure 10

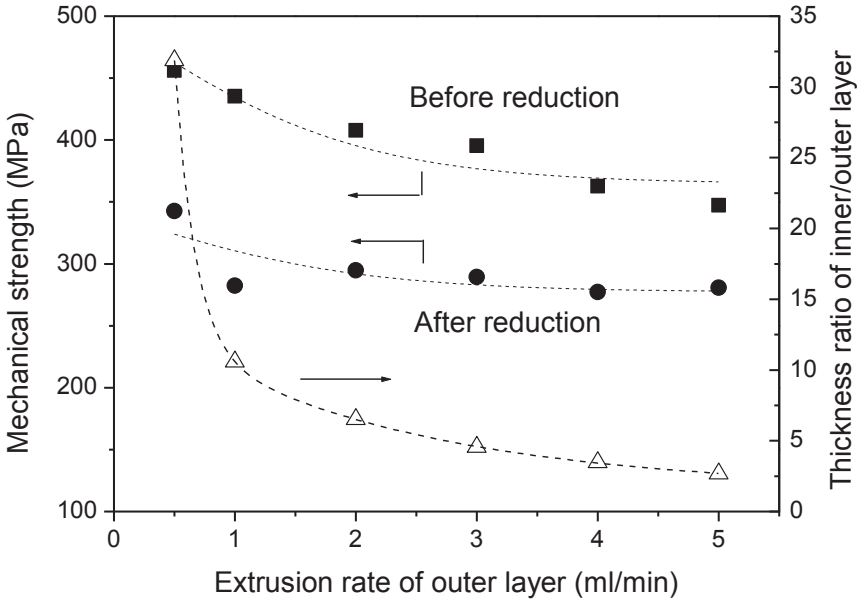
Mechanical strength (MPa)
Thickness ratio of inner/outer layer
Extrusion rate of outer layer (ml/min)
Before reduction
After reduction
500
400
300
200
100
35
30
25
20
15
10
5
0
0
1
2
3
4
5

Figure 11

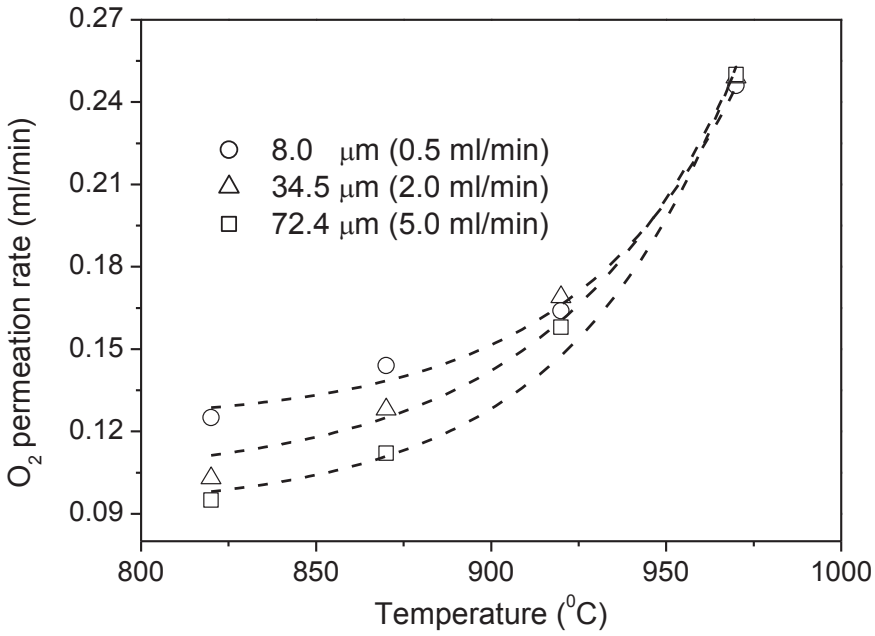
0.27
0.24
0.21
0.18
0.15
0.12
0.09
800
850
900
950
1000
O2 permeation rate (ml/min)
Temperature (0C)
8.0 μm (0.5 ml/min)
34.5 μm (2.0 ml/min)
72.4 μm (5.0 ml/min)

Figure 12

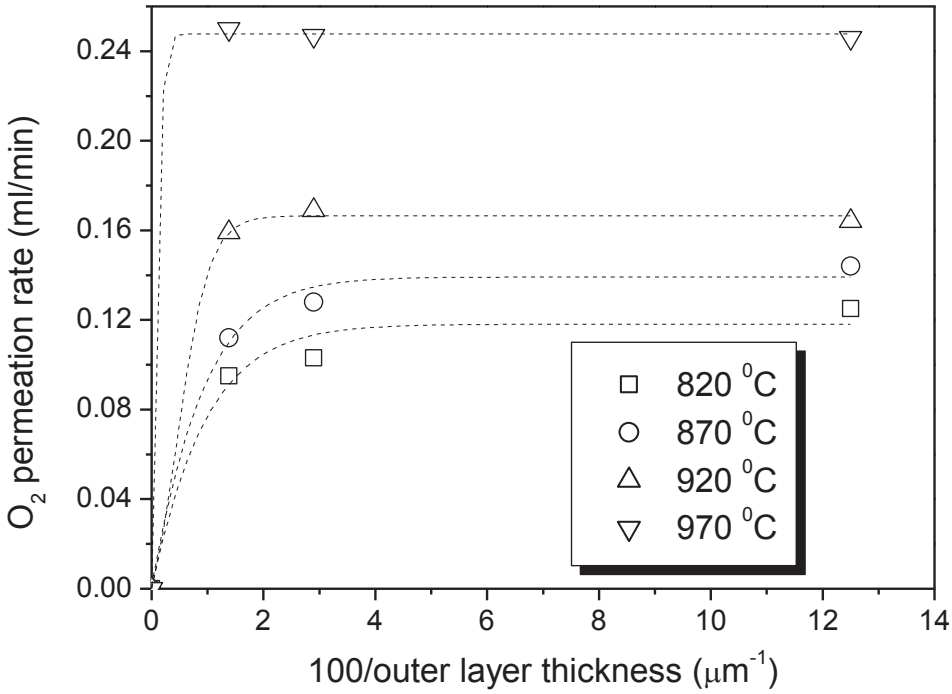
0.24
0.20
0.16
0.12
0.08
0.04
0.00
O_2 permeation rate (ml/min)
0
2
4
6
8
10
12
14
100/outer layer thickness (μm^{-1})
820 ^{0}C
870 ^{0}C
920 ^{0}C
970 ^{0}C

Figure 13

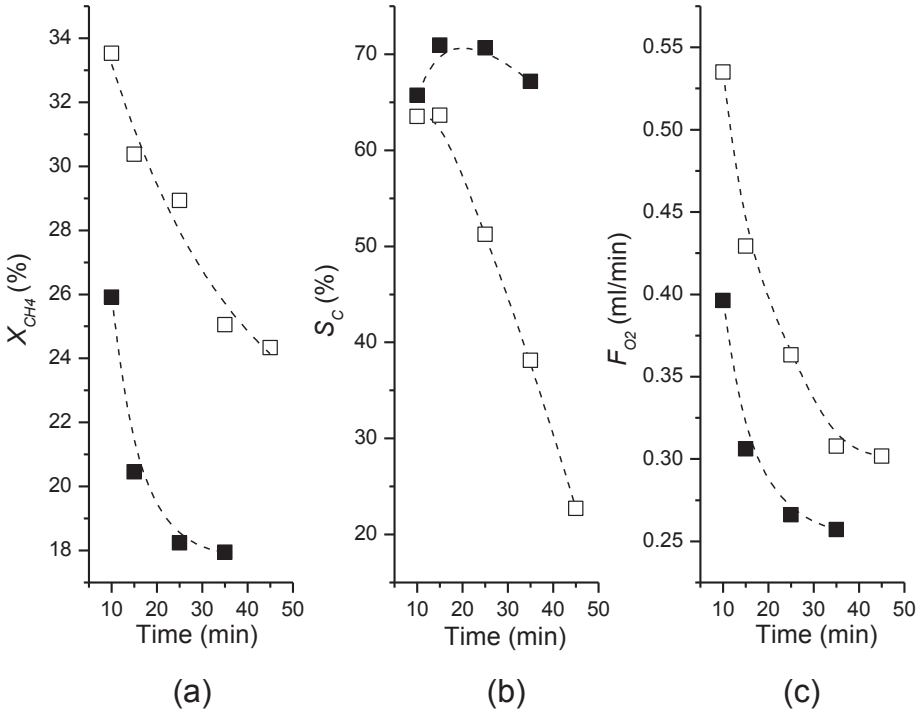

Figure 14